HIGH-TEMPERATURE PERIDOTITE MYLONITES REVEAL DEEP ORGANIC CARBON CYCLE AT OCEANIC TRANSFORM FAULTS

- Suzanne JOANNO -

Supervisors : Cécile Prigent, Manon Bickert, Bénédicte Ménez & Muriel Andreani

Team: LOMs et Géosciences Marines

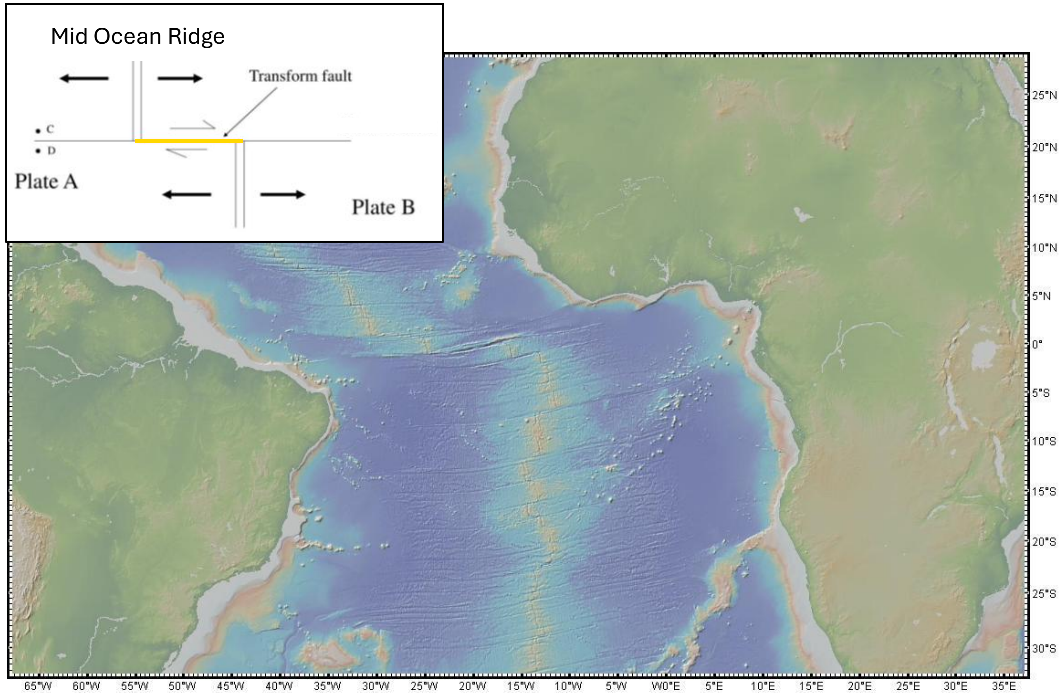

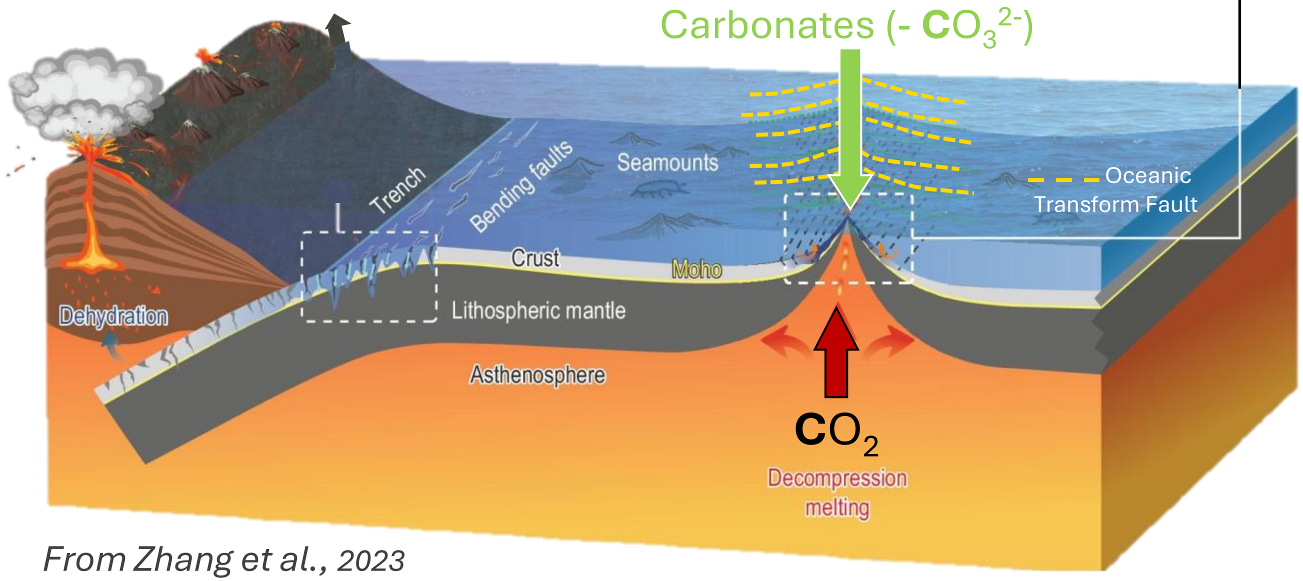

From Zhang et al., 2023

Serpentinization reation

$$6[(Mg,Fe)_2SiO_4] + 7H_2O \rightarrow 3[Mg_3Si_2O_5(OH)_4] + Fe_3O_4 + H_2$$

olivine + *water* → ***serpentine*** + *magnetite* + *hydrogen*

Andreani et al., 2023

Abiotic reaction

$$CO_2 + 4H_2 \leftrightarrows CH_4 + 2H_2O$$

Inorganic

Organic

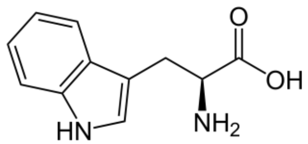

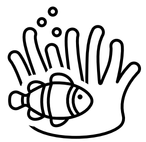

Fluid circulation

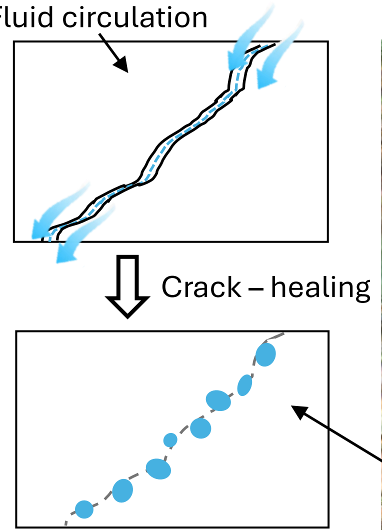

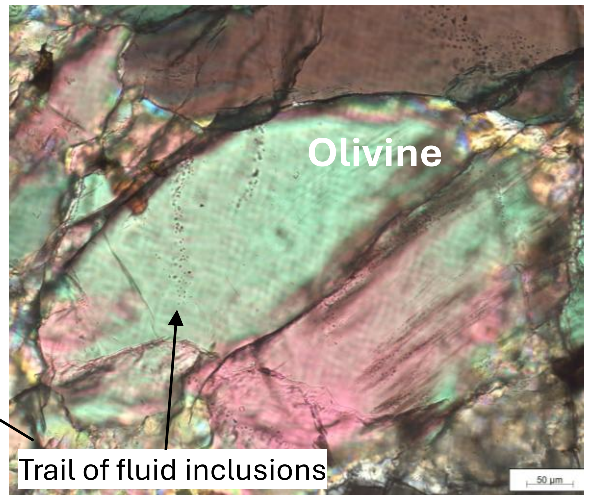

Trail of fluid inclusions

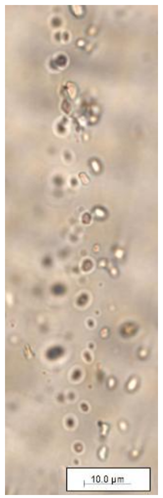

Serpentinization reation

$$6[(Mg,Fe)_2SiO_4] + 7H_2O \rightarrow 3[Mg_3Si_2O_5(OH)_4] + Fe_3O_4 + H_2$$

olivine + *water* → ***serpentine*** + *magnetite* + *hydrogen*

Andreani et al., 2023

Abiotic reaction

$$CO_2 + 4H_2 \leftrightarrows CH_4 + 2H_2O$$

Inorganic

Organic

Oceanic Transform Fault ?

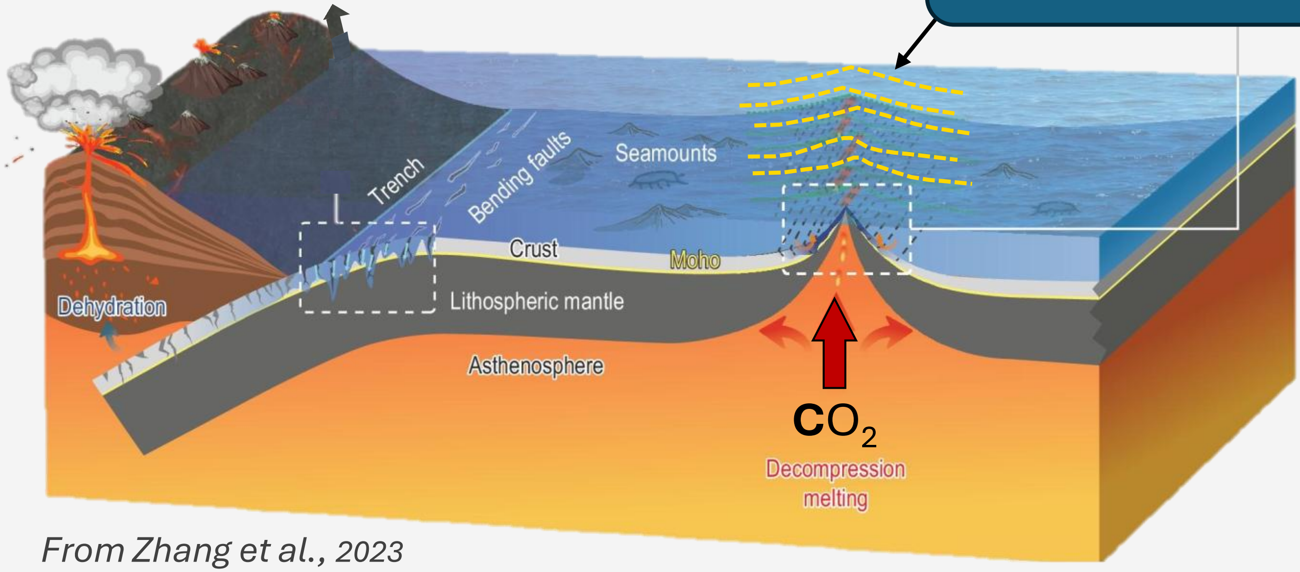

From Zhang et al., 2023

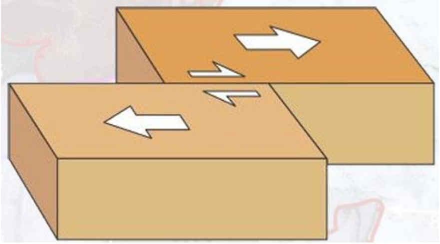

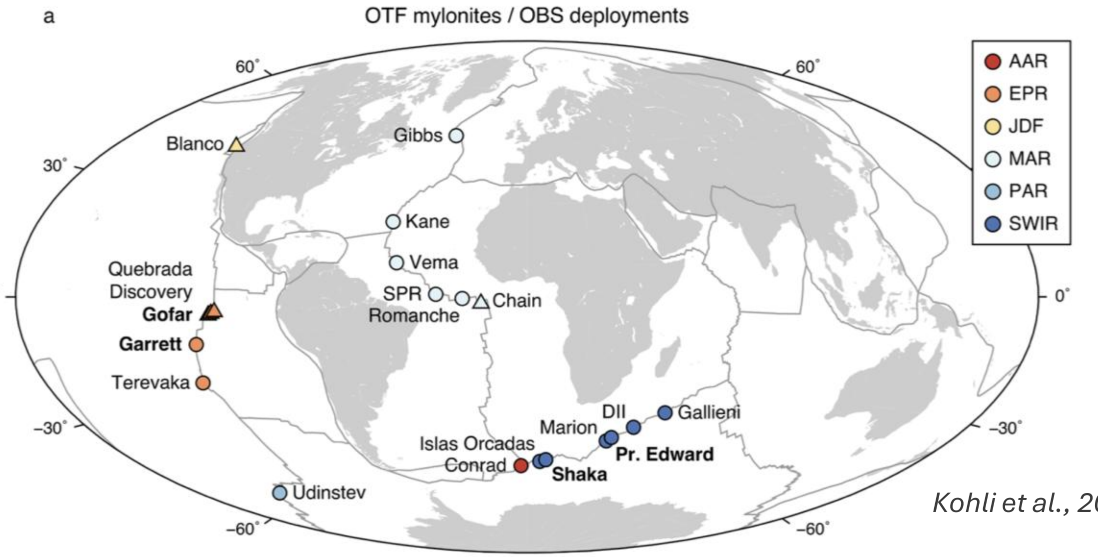

Kohli et al., 2021

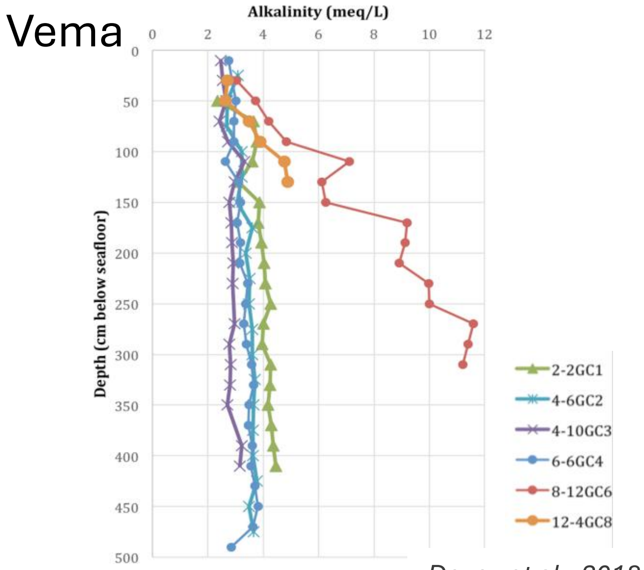

Devey et al., 2018

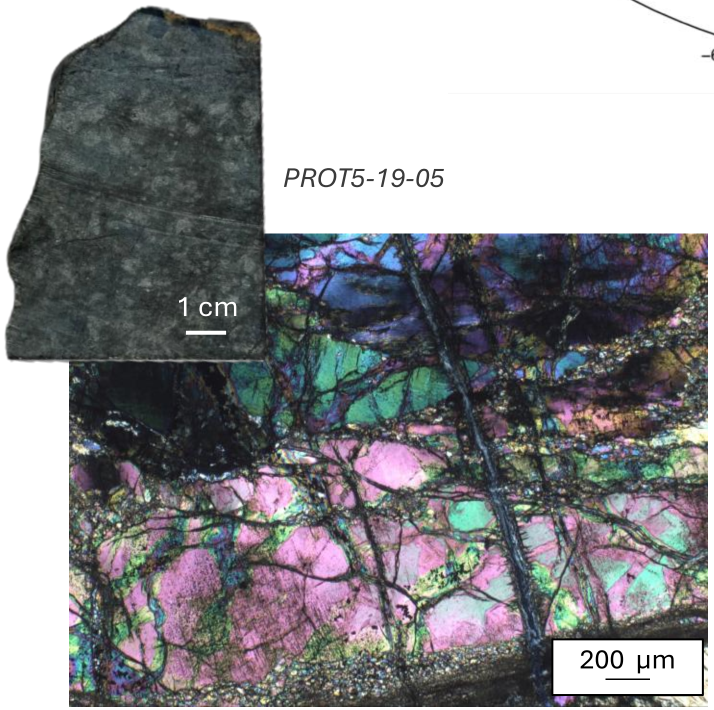

PROT5-19-05

HT-mylonite PROT5-19-01

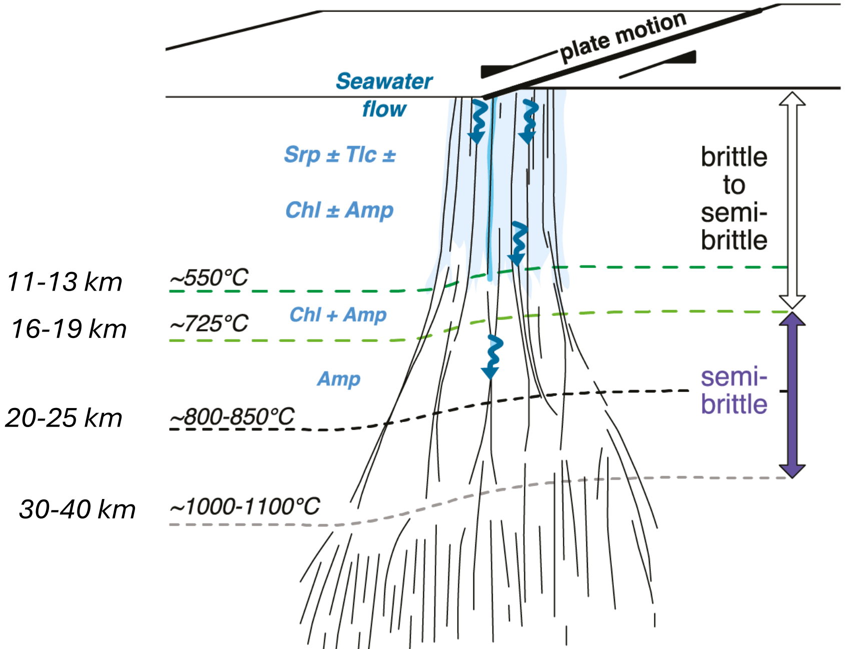

Prigent et al., 2020

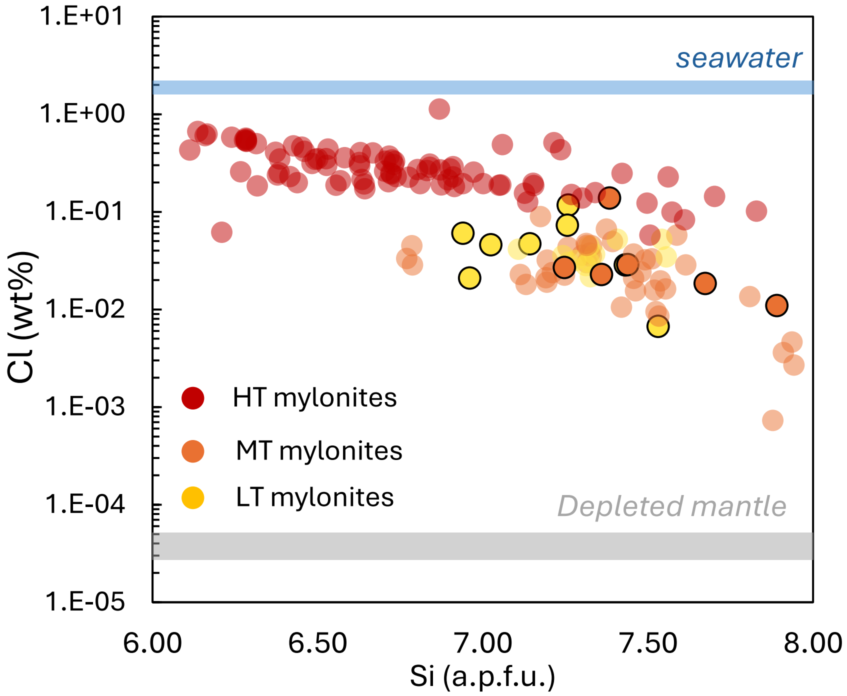

Data from Prigent et al., 2020 *Data from S.Joanno, 2024*

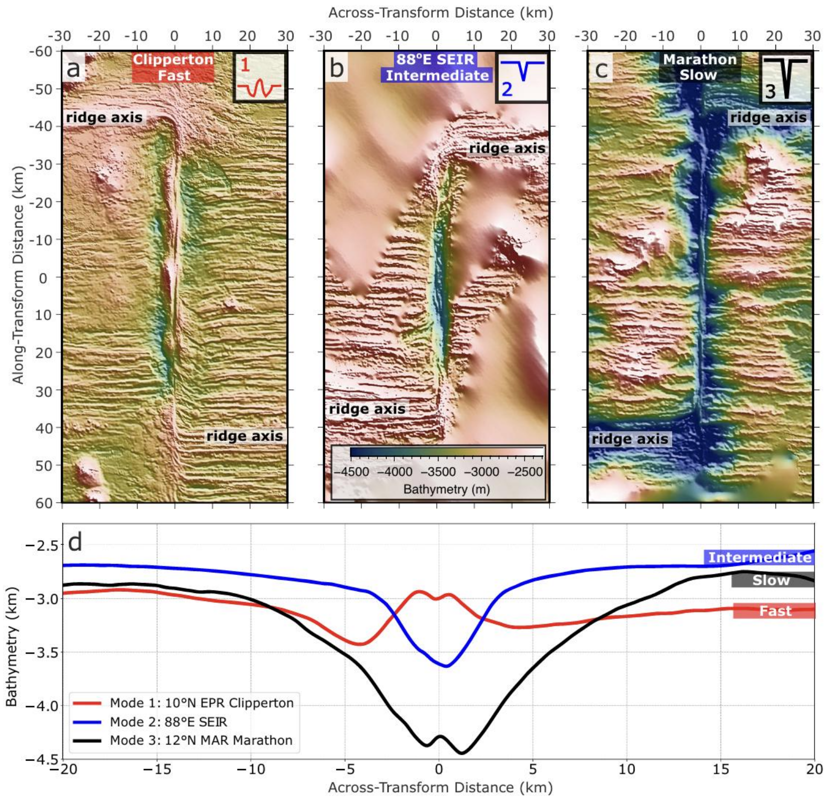

Tian et al., 2024

Carbonates (-CO_3^{2-})

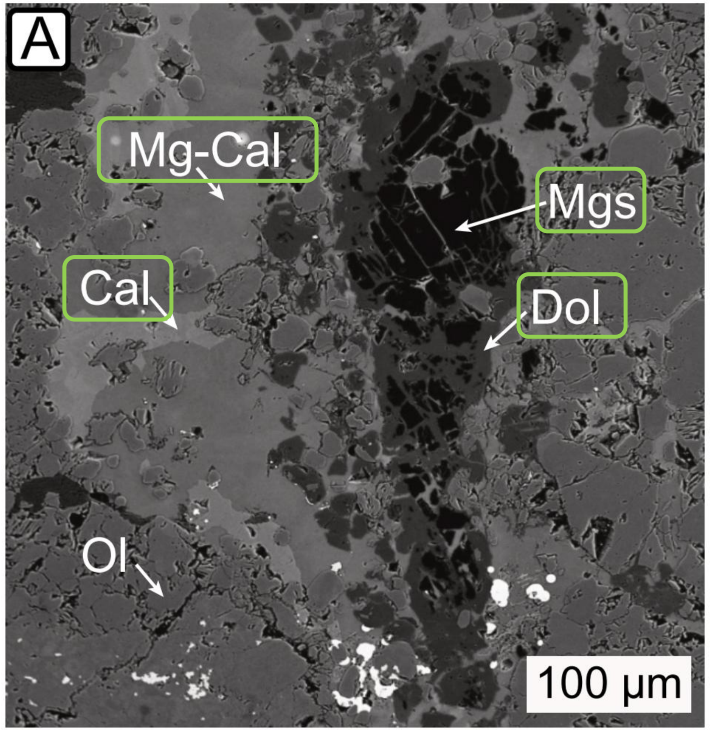

Klein et al., 2024

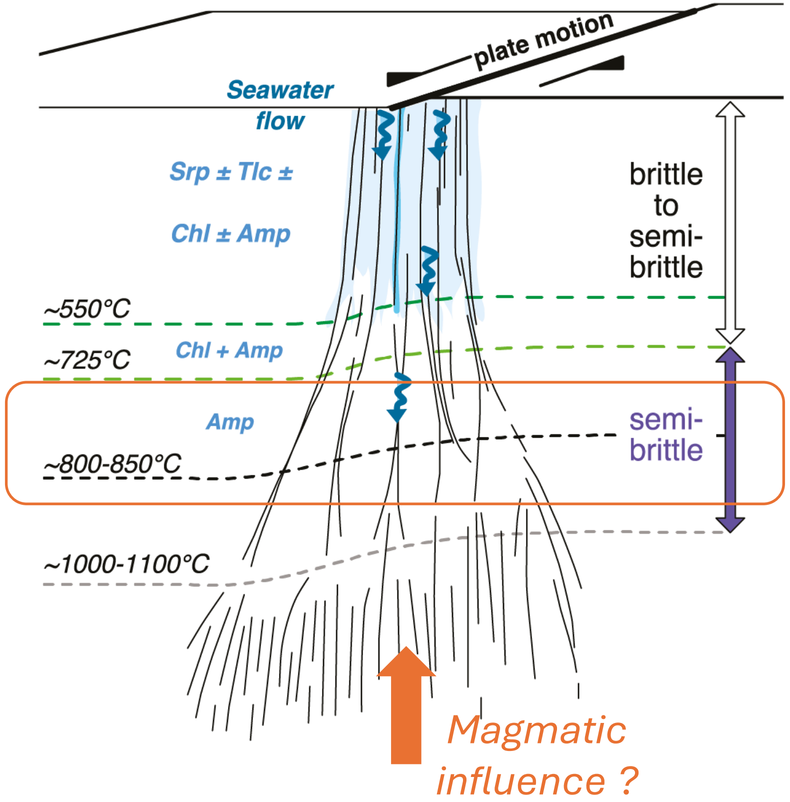

Prigent et al., 2020

Source of fluids percolating in transform faults and variation with spreading rate?

Volatile & Deep carbon cycles?

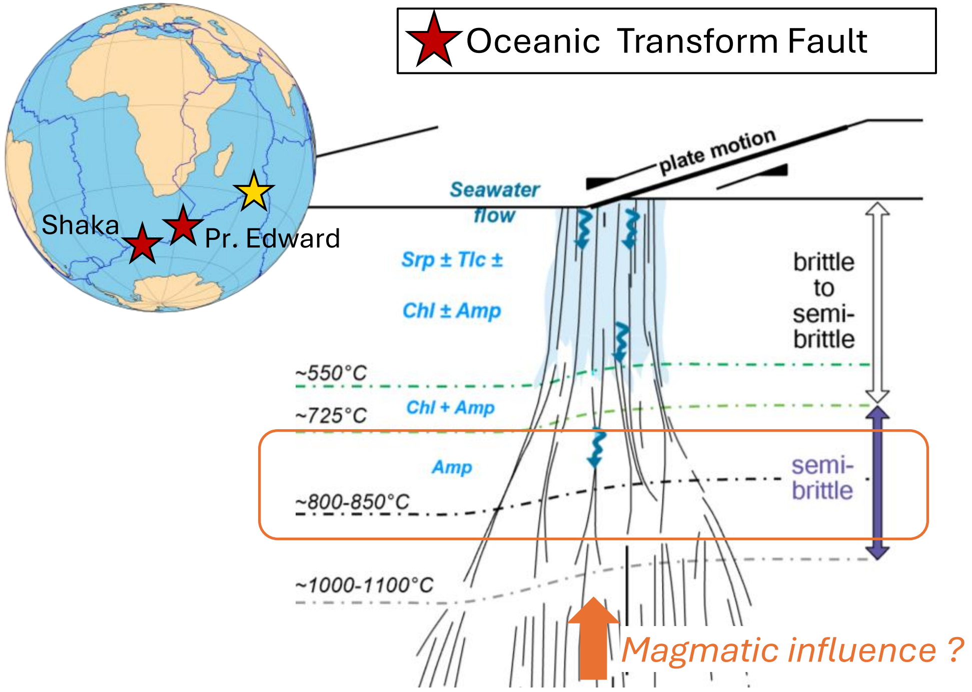

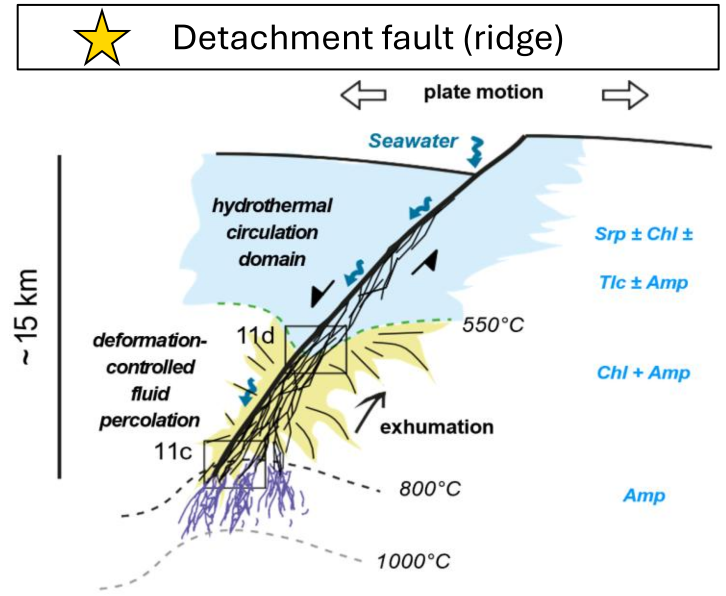

1 Hydrated phases

- → Optical and electronic microscopy
- → EPMA
- → ICP-MS laser

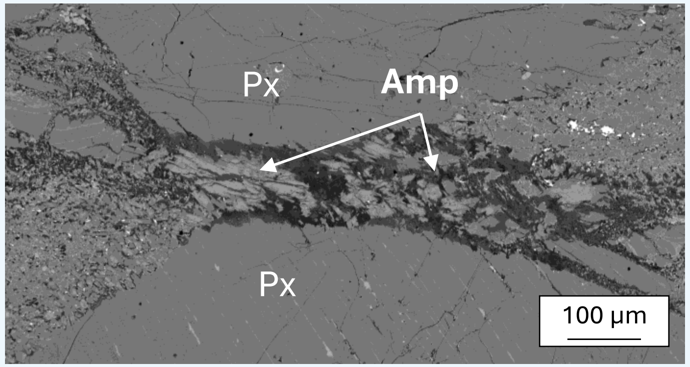

2 **Fluid Inclusions (FI)**

- → Optical microsopy
- → Raman microscopy
- → FIB-SEM

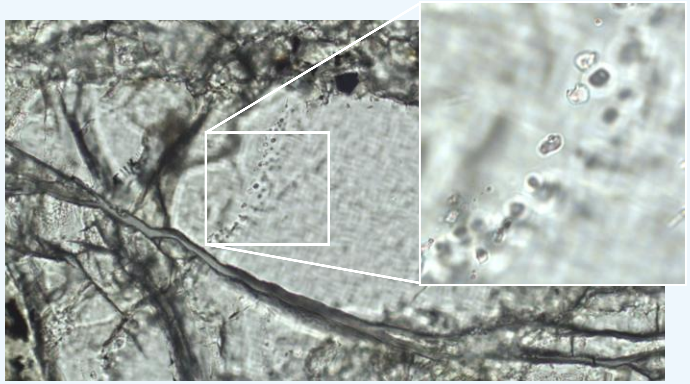

3 Matrix

- → Fourrier Transform Infra Red (FTIR)
- → Electronic microscopy

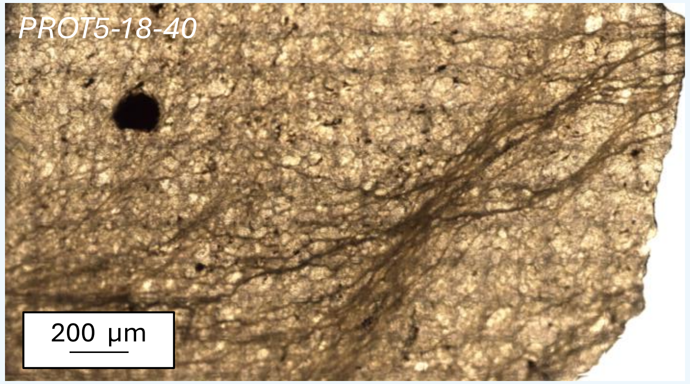

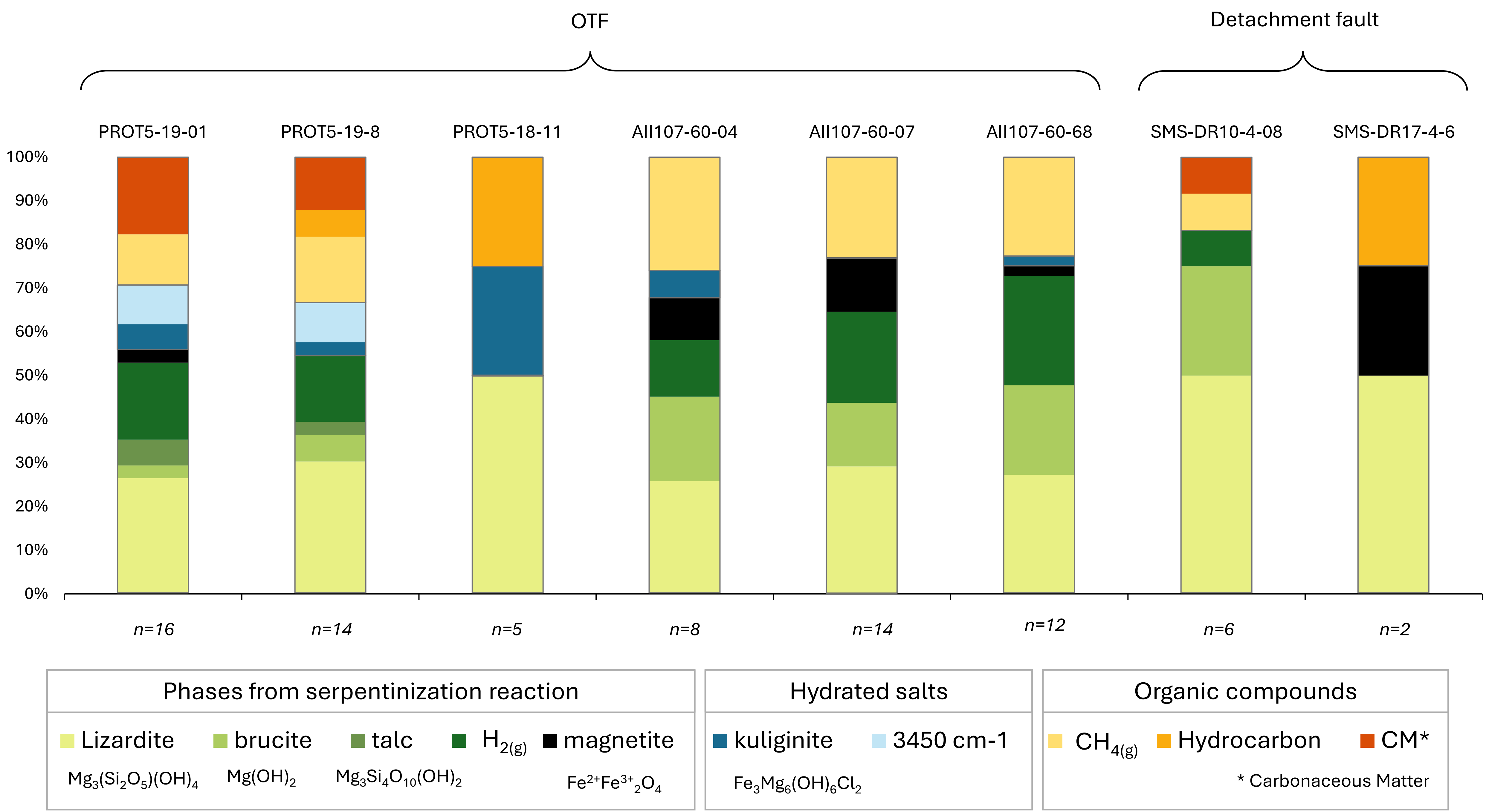

OTF
Detachment fault
PROT5-19-01
PROT5-19-8
PROT5-18-11
AII107-60-04
AII107-60-07
AII107-60-68
SMS-DR10-4-08
SMS-DR17-4-6
100%
90%
80%
70%
60%
50%
40%
30%
20%
10%
0%
n=16
n=14
n=5
n=8
n=14
n=12
n=6
n=2
Phases from serpentinization reaction
Lizardite
brucite
talc
$H_{2(g)}$
magnetite
$Mg_3(Si_2O_5)(OH)_4$
$Mg(OH)_2$
$Mg_3Si_4O_{10}(OH)_2$
$Fe^{2+}Fe^{3+}{}_2O_4$
Hydrated salts
kuliginite
3450 cm-1
$Fe_3Mg_6(OH)_6Cl_2$
Organic compounds
$CH_{4(g)}$
Hydrocarbon
CM*
* Carbonaceous Matter

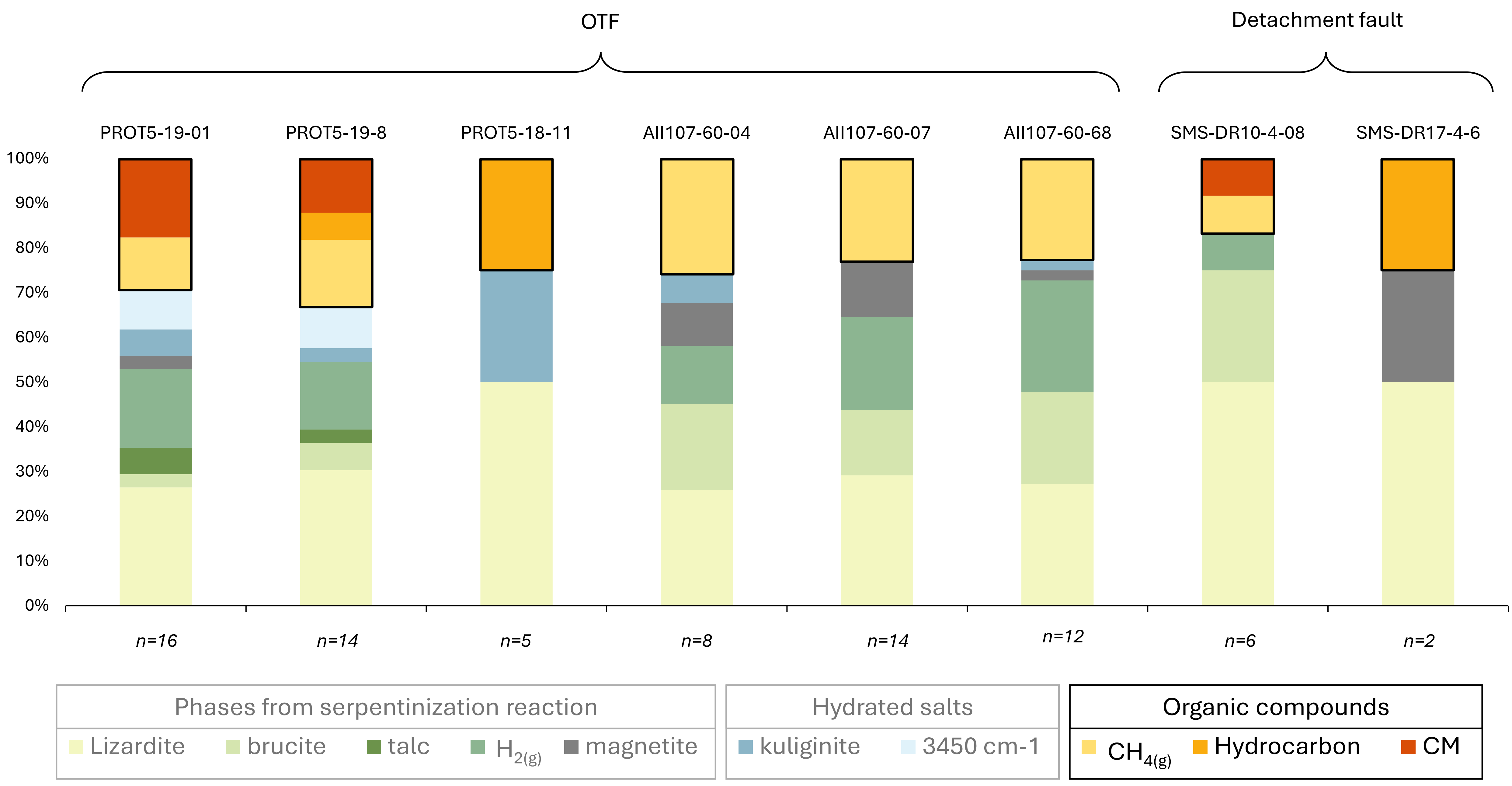

OTF
Detachment fault
PROT5-19-01
PROT5-19-8
PROT5-18-11
AII107-60-04
AII107-60-07
AII107-60-68
SMS-DR10-4-08
SMS-DR17-4-6
100%
90%
80%
70%
60%
50%
40%
30%
20%
10%
0%
n=16
n=14
n=5
n=8
n=14
n=12
n=6
n=2
Phases from serpentinization reaction
Lizardite
brucite
talc
$H_{2(g)}$
magnetite
Hydrated salts
kuliginite
3450 cm-1
Organic compounds
$CH_{4(g)}$
Hydrocarbon
CM

Modified from Andreani et al., 2023

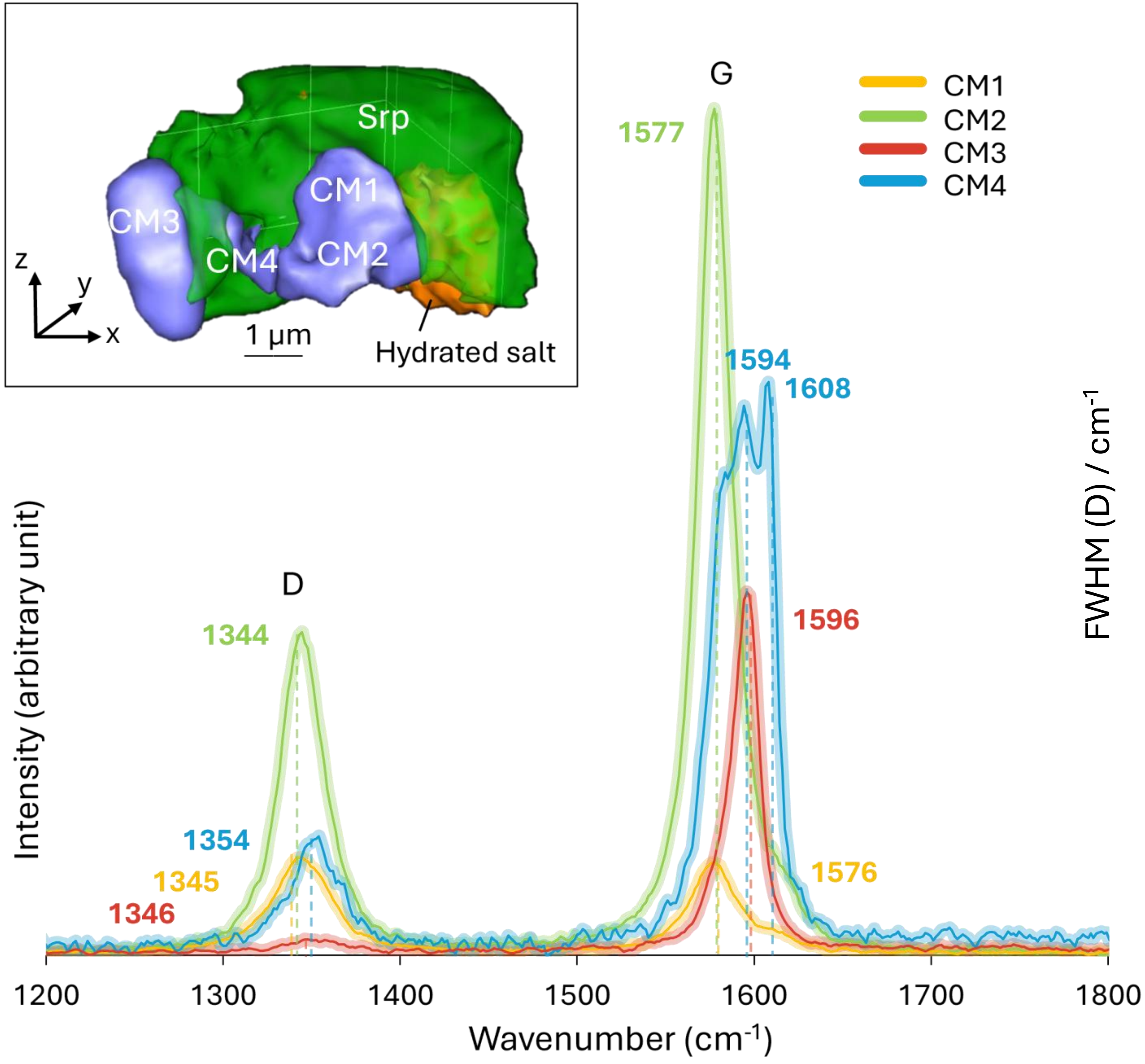

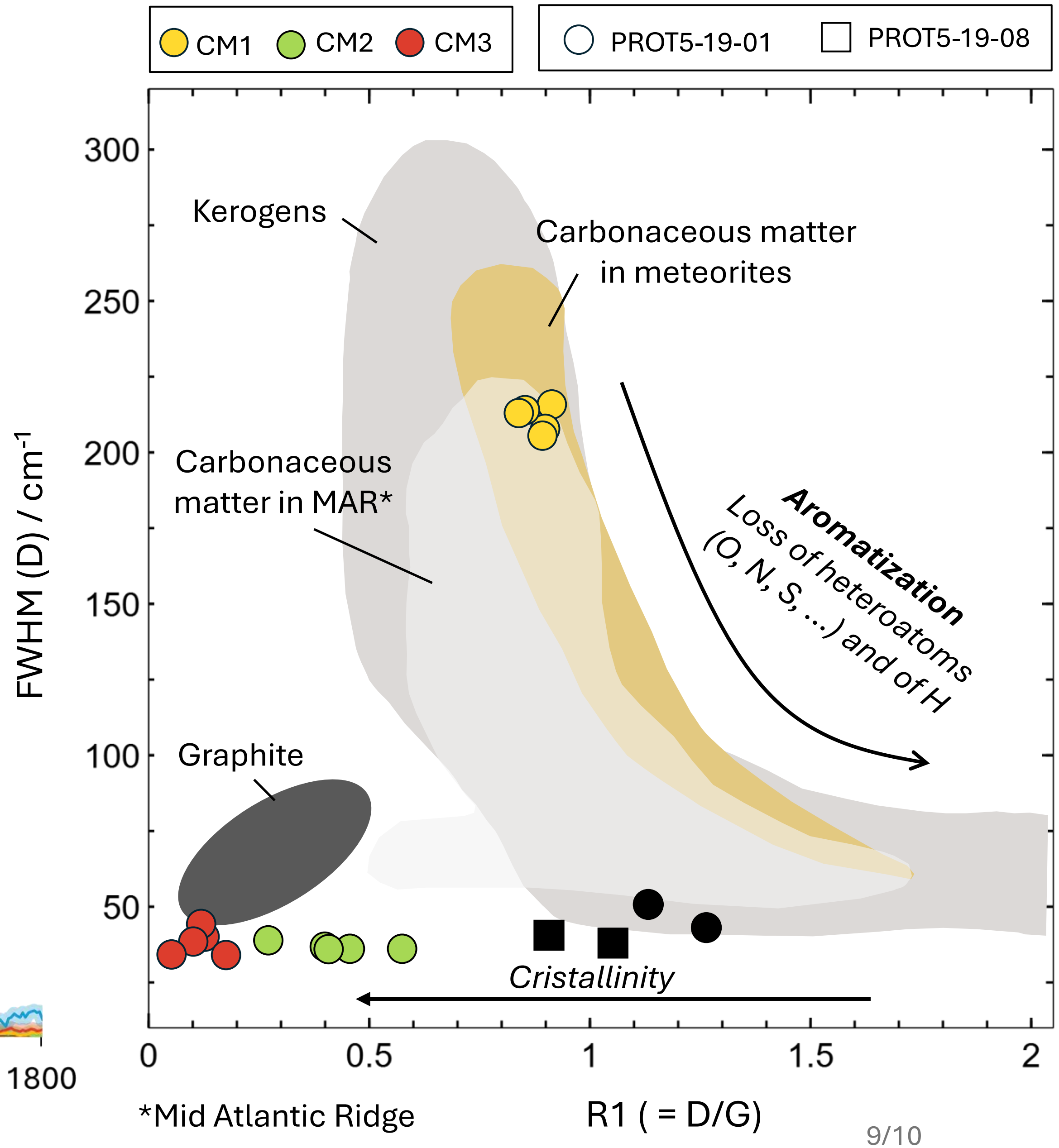

*Mid Atlantic Ridge

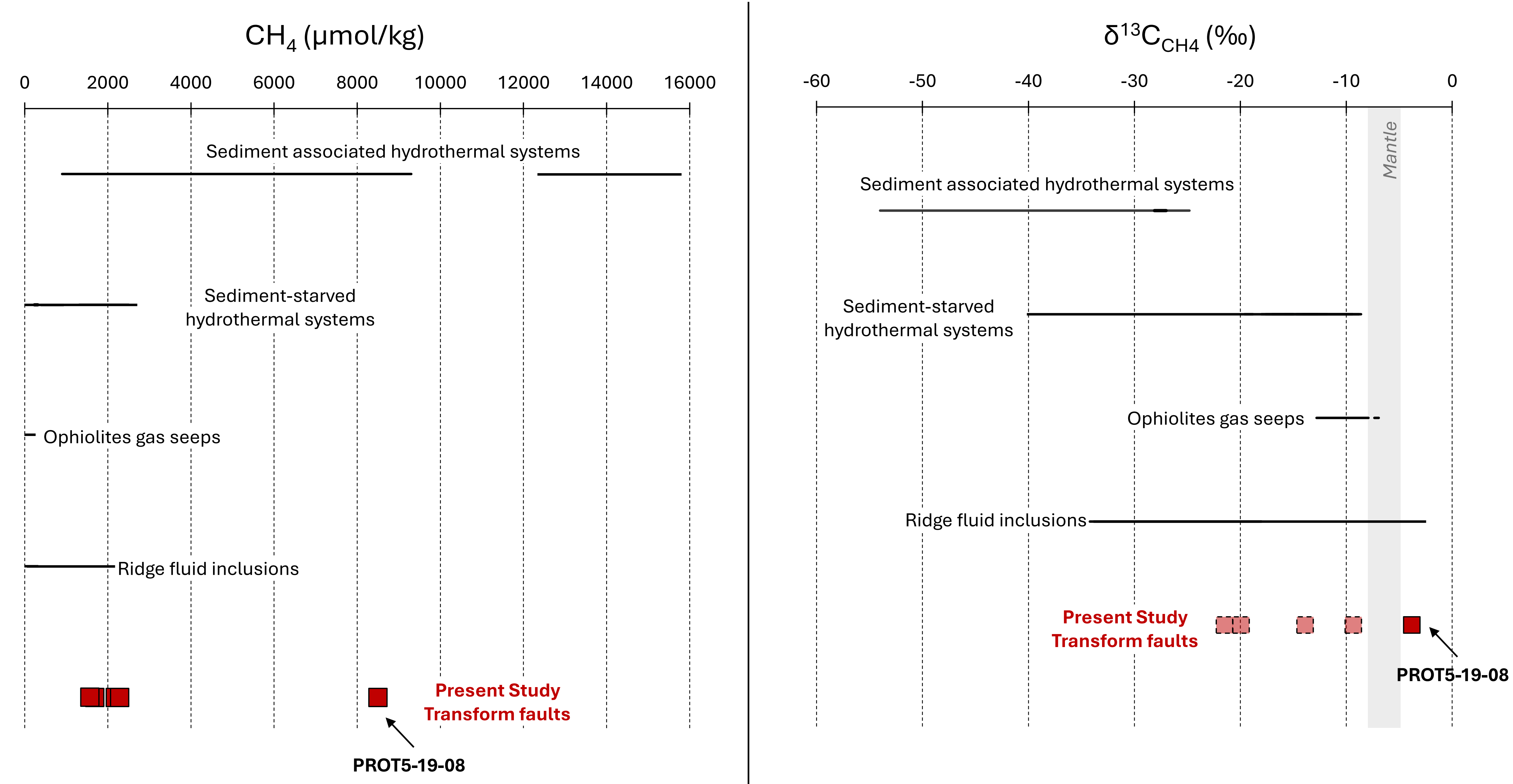

Modified from Prakash et al., 2022

What's next ?

Carbon-rich fluid circulation

Favorable environments for abiotic organic synthesis

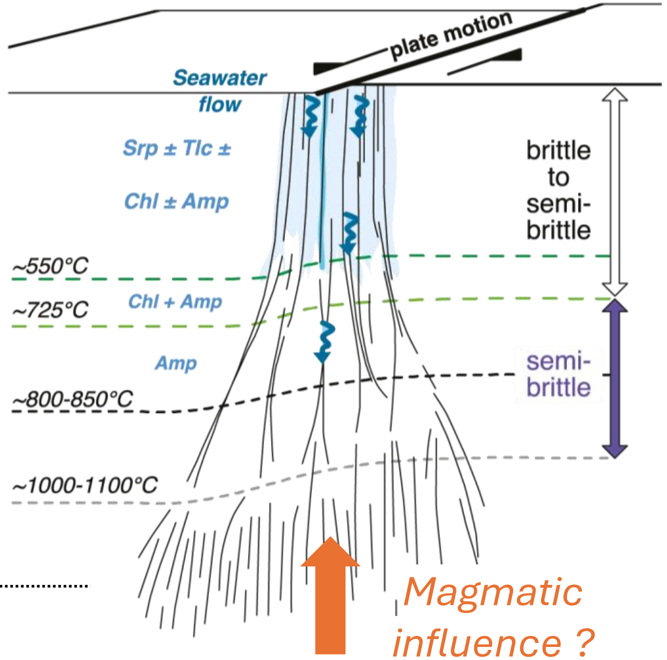

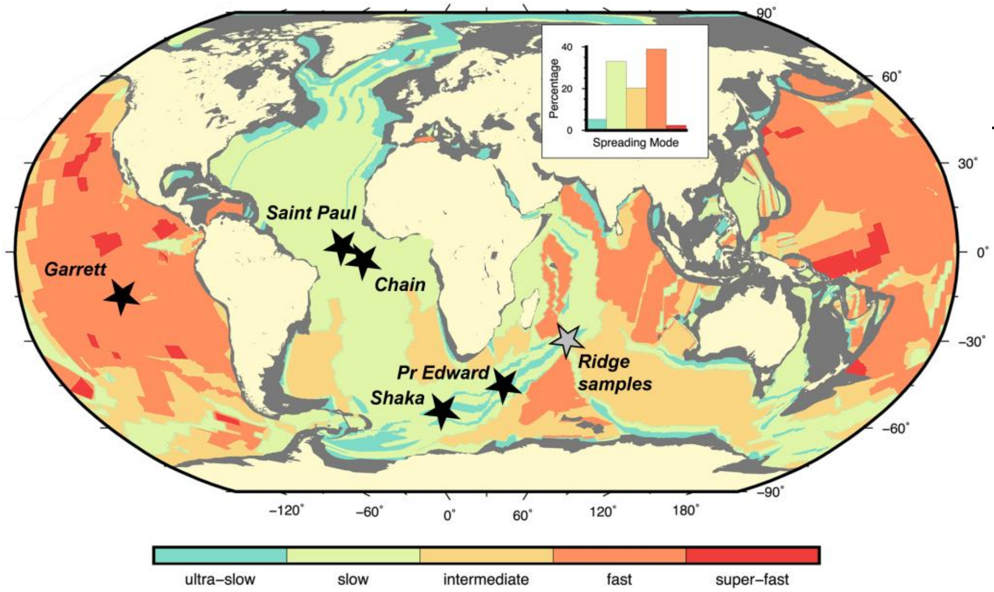

Formation mechanisms?
Role of magmatism? Hydrothermalism? Deformation?

Diversity of organic compounds in transform faults ?

References

Andreani, M. *et al.* (2023) « The rocky road to organics needs drying », *Nature Communications*, 14(1), p. 347. Disponible sur: https://doi.org/10.1038/s41467-023-36038-6.

Andreani, M. et Ménez, B. (2019) « New Perspectives on Abiotic Organic Synthesis and Processing during Hydrothermal Alteration of the Oceanic Lithosphere », in B.N. Orcutt, I. Daniel, et R. Dasgupta (éd.) *Deep Carbon*. 1re éd. Cambridge University Press, p. 447-479. Disponible sur: https://doi.org/10.1017/9781108677950.015.

Bickert, M., Cannat, M. et Brunelli, D. (2023) « Hydrous fluids down to the semi-brittle root zone of detachment faults in nearly amagmatic ultra-slow spreading ridges », *Lithos*, 442-443, p. 107084. Disponible sur: https://doi.org/10.1016/j.lithos.2023.107084.

Devey, C.W. *et al.* (2018) « Habitat characterization of the Vema Fracture Zone and Puerto Rico Trench », *Deep Sea Research Part II: Topical Studies in Oceanography*, 148, p. 7-20. Disponible sur: https://doi.org/10.1016/j.dsr2.2018.02.003.

Klein, F. *et al.* (2024) « Mineral carbonation of peridotite fueled by magmatic degassing and melt impregnation in an oceanic transform fault », *Proceedings of the National Academy of Sciences*, 121(8), p. e2315662121. Disponible sur: https://doi.org/10.1073/pnas.2315662121.

Klein, F., Grozeva, N.G. et Seewald, J.S. (2019) « Abiotic methane synthesis and serpentinization in olivine-hosted fluid inclusions », *Proceedings of the National Academy of Sciences*, 116(36), p. 17666-17672. Disponible sur: https://doi.org/10.1073/pnas.1907871116.

Kohli, A. *et al.* (2021) « Oceanic transform fault seismicity and slip mode influenced by seawater infiltration », *Nature Geoscience*, 14(8), p. 606-611. Disponible sur: https://doi.org/10.1038/s41561-021-00778-1.

Prigent, C. *et al.* (2020) « Fracture-mediated deep seawater flow and mantle hydration on oceanic transform faults », *Earth and Planetary Science Letters*, 532, p. 115988. Disponible sur: https://doi.org/10.1016/j.epsl.2019.115988.

Sforna, M.C. *et al.* (2018) « Abiotic formation of condensed carbonaceous matter in the hydrating oceanic crust », *Nature Communications*, 9(1), p. 5049. Disponible sur: https://doi.org/10.1038/s41467-018-07385-6.

Surya Prakash, L. *et al.* (2022) « Volatile-Rich Hydrothermal Plumes Over the Southern Central Indian Ridge, 24°49'S: Evidence for a New Hydrothermal Field Hosted by Ultramafic Rocks », *Geochemistry, Geophysics, Geosystems*, 23(10), p. e2022GC010452. Disponible sur: https://doi.org/10.1029/2022GC010452.

Tian, X. *et al.* (2024) « Magmatism controls global oceanic transform fault topography », *Nature Communications*, 15(1), p. 1914. Disponible sur: https://doi.org/10.1038/s41467-024-46197-9.

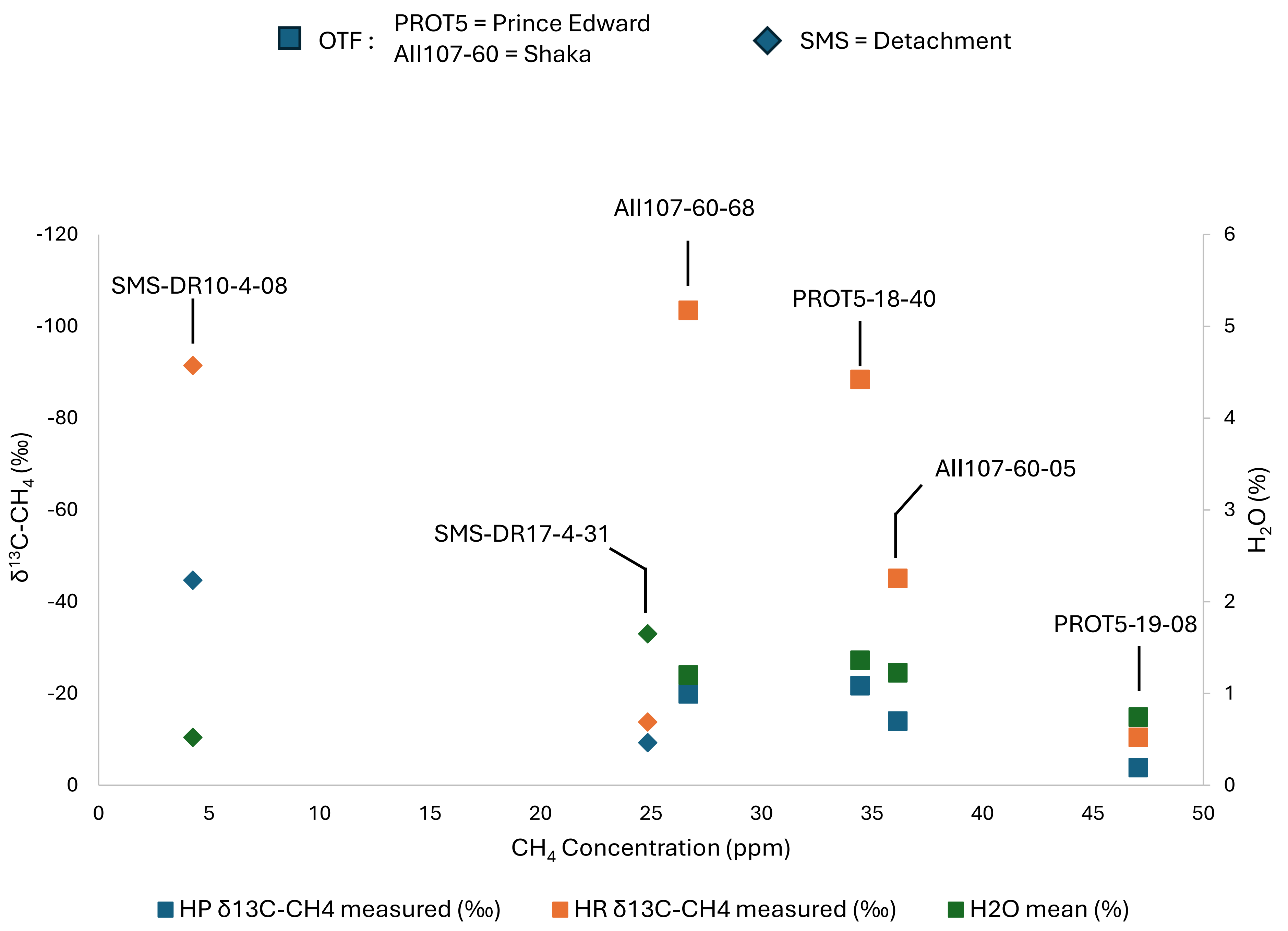
OTF :
PROT5 = Prince Edward
AII107-60 = Shaka
SMS = Detachment
AII107-60-68
SMS-DR10-4-08
PROT5-18-40
AII107-60-05
SMS-DR17-4-31
PROT5-19-08
-120
-100
-80
-60
-40
-20
0
6
5
4
3
2
1
0
δ13C-CH4 (‰)
H2O (%)
0
5
10
15
20
25
30
35
40
45
50
CH4 Concentration (ppm)
HP δ13C-CH4 measured (‰)
HR δ13C-CH4 measured (‰)
H2O mean (%)

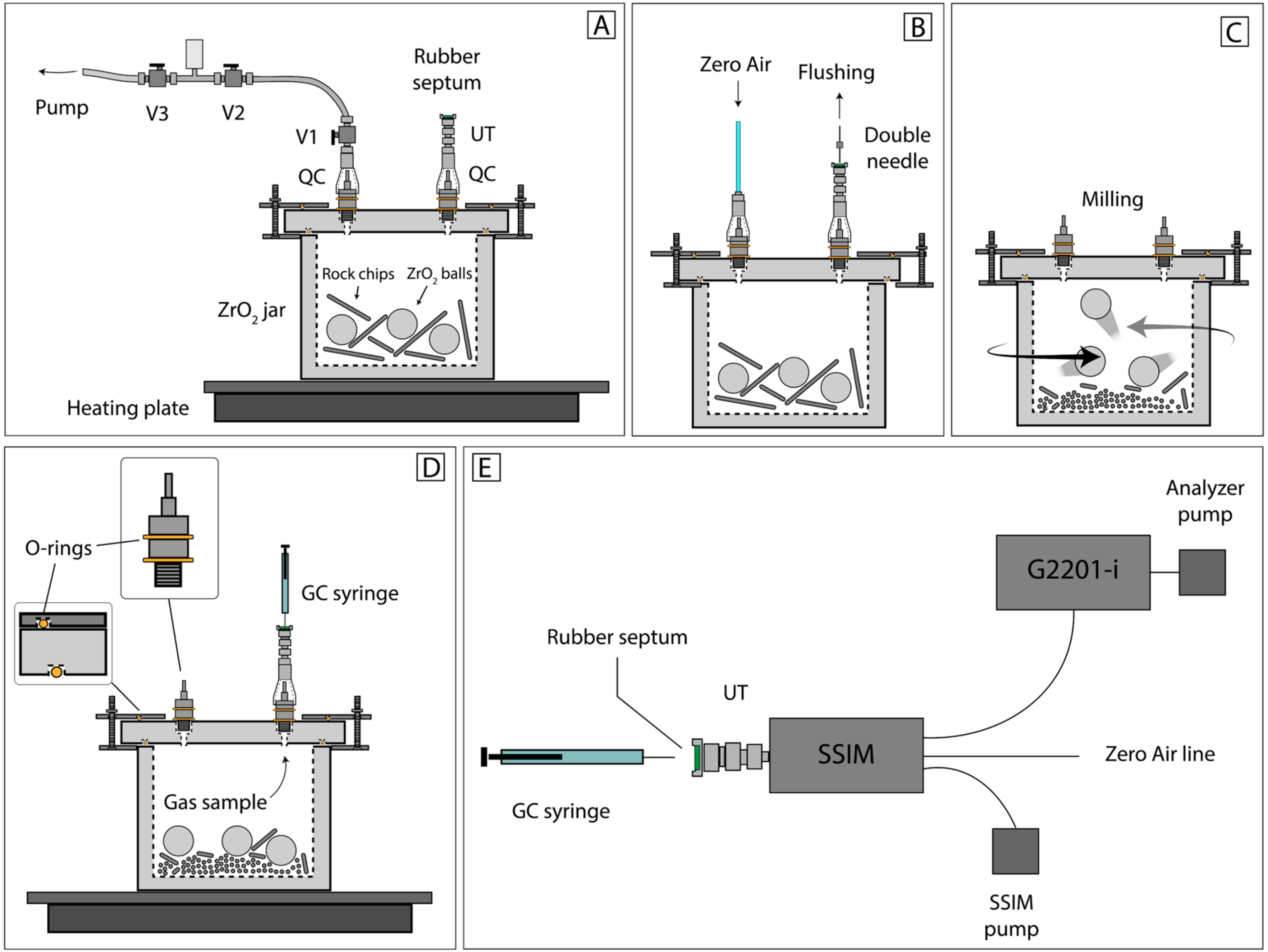

Olivieri et al., 2024

6 samples :

- 2x Shaka transform fault;
- 2x Prince Edward transform fault ;
- 2x detachment fault

Reliable measurments when CH_4 concentrations = 40-50 ppm

Picarro analyzer = 2 modes:

- **High Precision (HP)**
- High Range (HR)

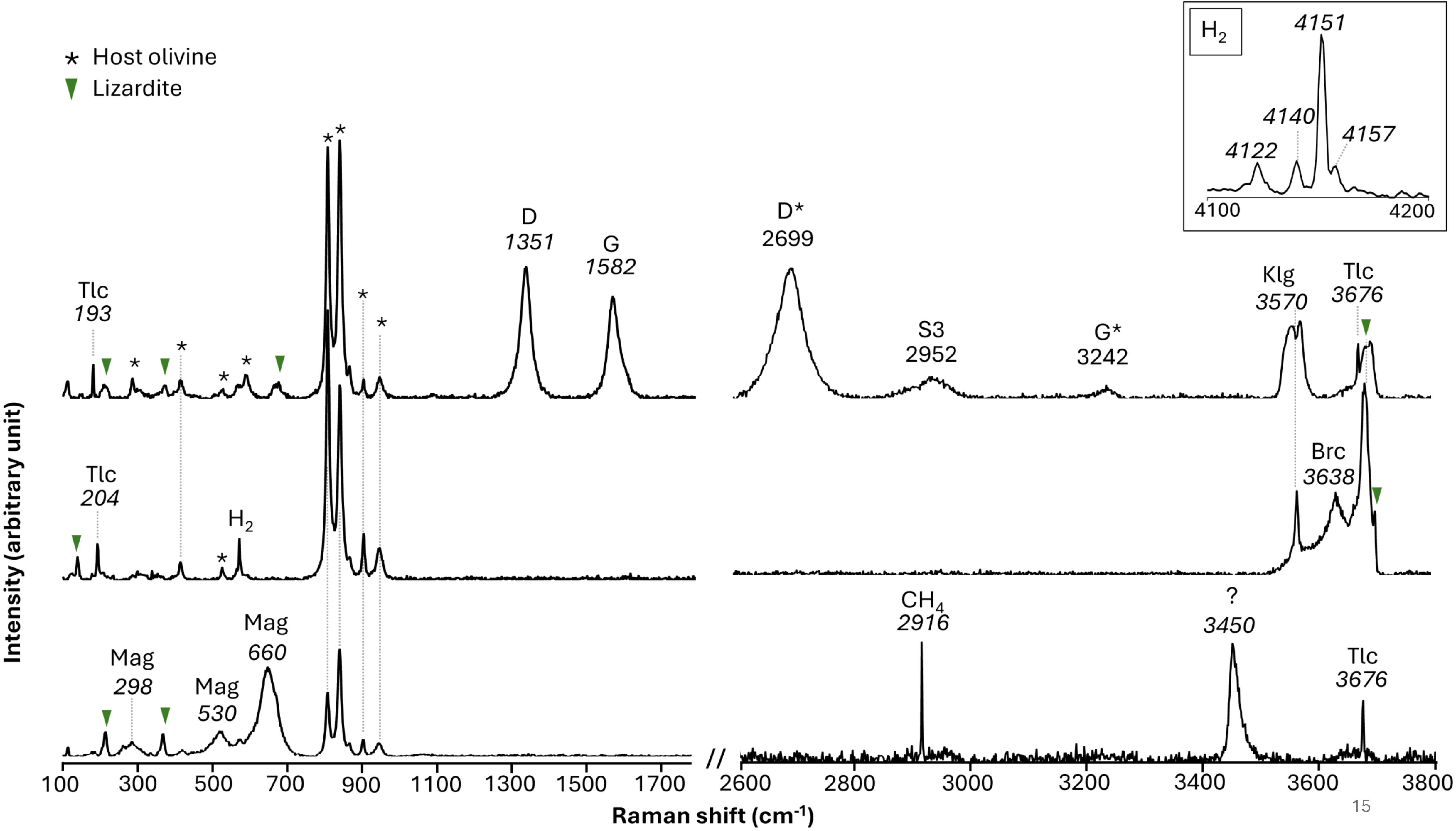

* Host olivine
Lizardite
H2
4151
4140
4157
4122
4100
4200
D
1351
G
1582
D*
2699
Tlc
193
S3
2952
G*
3242
Klg
3570
Tlc
3676
Tlc
204
H2
Brc
3638
Mag
298
Mag
530
Mag
660
CH4
2916
?
3450
Tlc
3676
Intensity (arbitrary unit)
100
300
500
700
900
1100
1300
1500
1700
2600
2800
3000
3200
3400
3600
3800
Raman shift (cm-1)

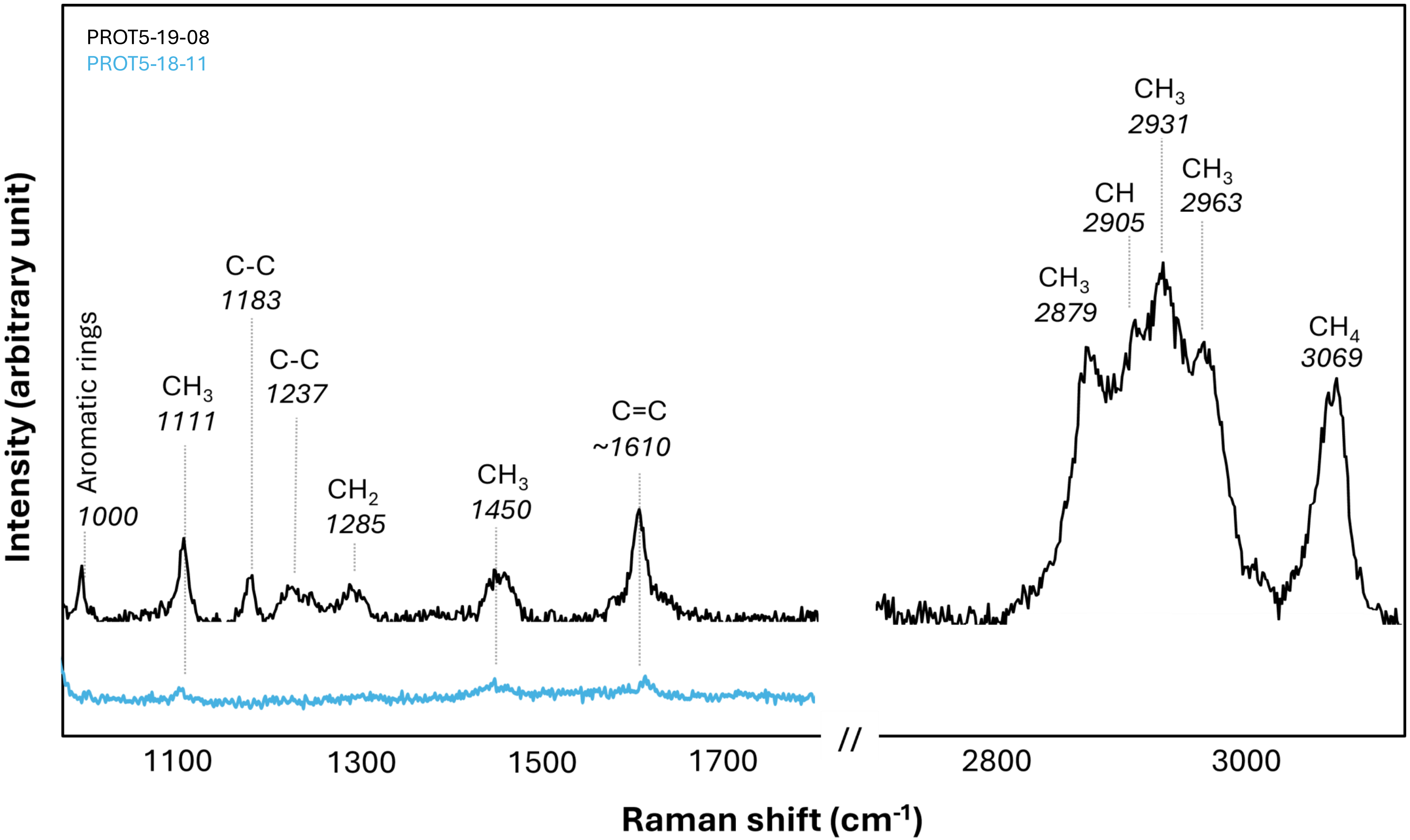

PROT5-19-08
PROT5-18-11
Intensity (arbitrary unit)
Raman shift (cm⁻¹)
Aromatic rings
1000
CH3
1111
C-C
1183
C-C
1237
CH2
1285
CH3
1450
C=C
~1610
CH3
2879
CH
2905
CH3
2931
CH3
2963
CH4
3069
1100
1300
1500
1700
//
2800
3000

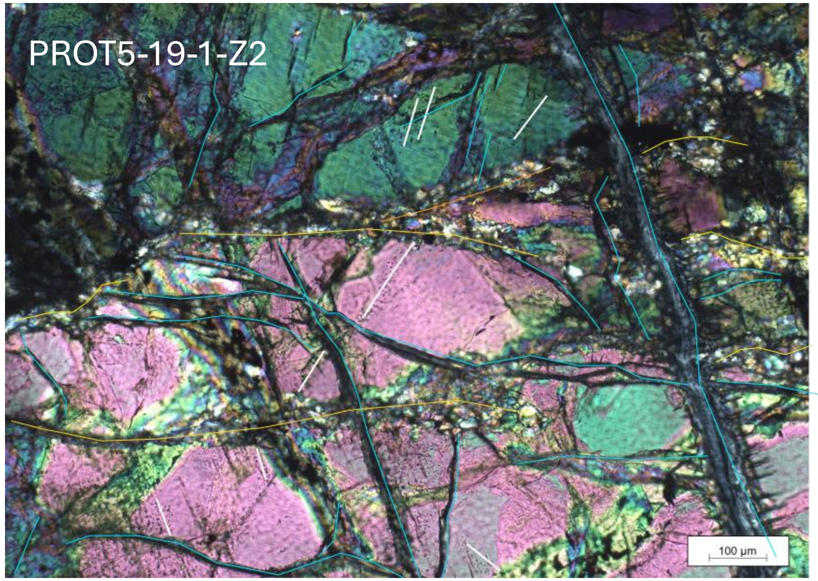

Fractures (BT)

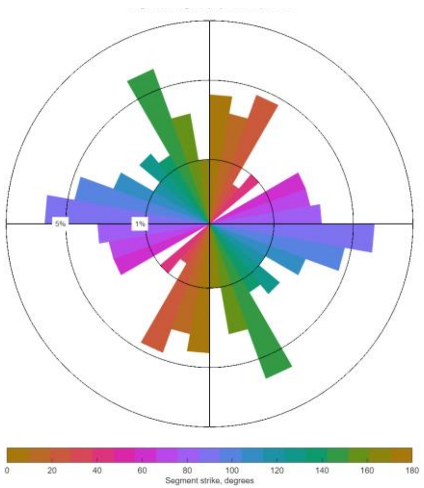

SZ (HT)

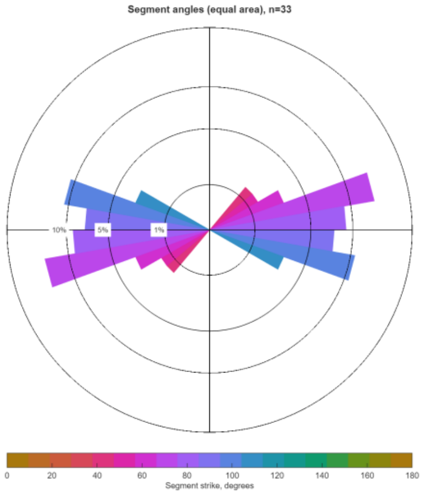

IF trails

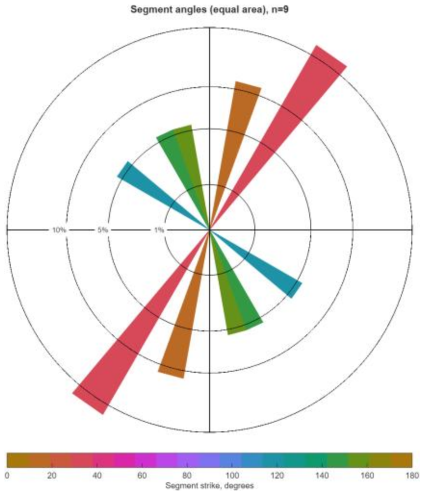

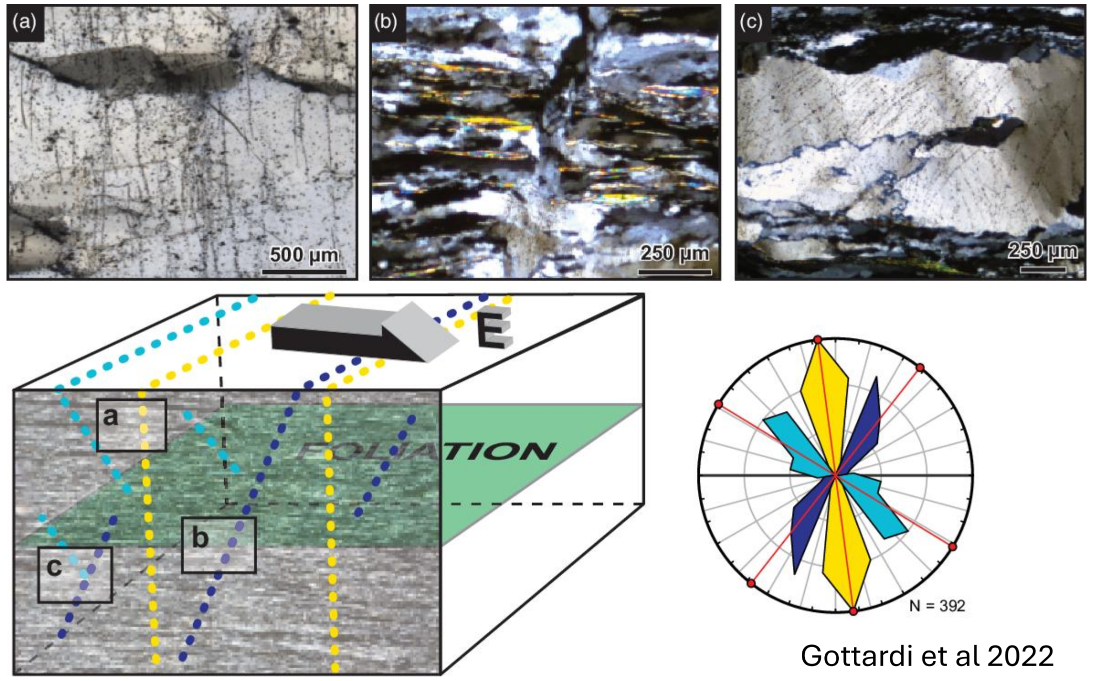

Gottardi et al 2022

PROT5-19-1 (SWIR TF)

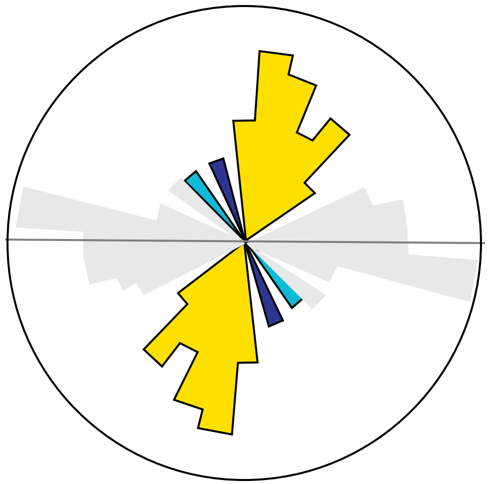

OTF

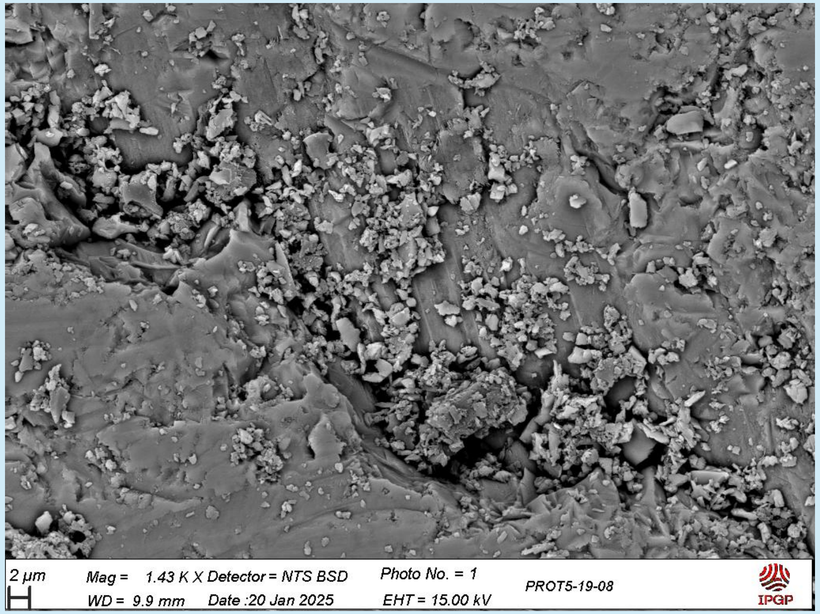

Detachment faults

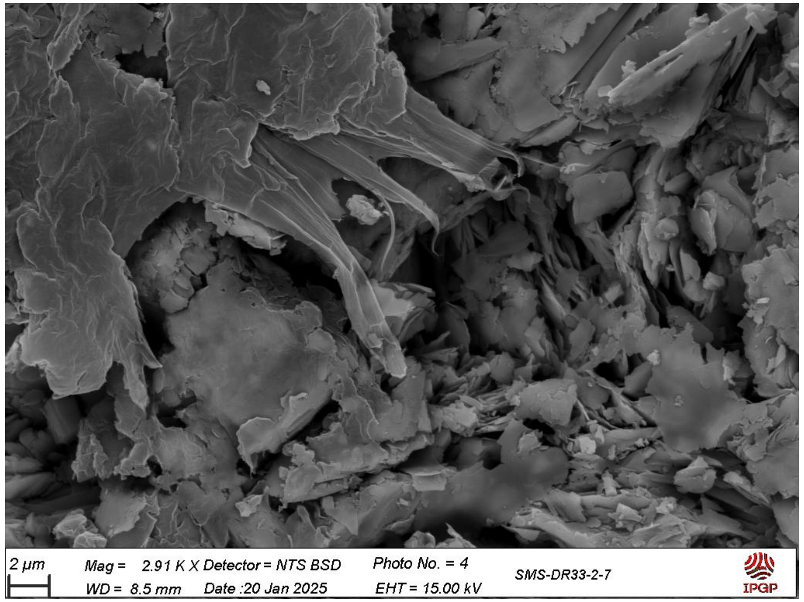

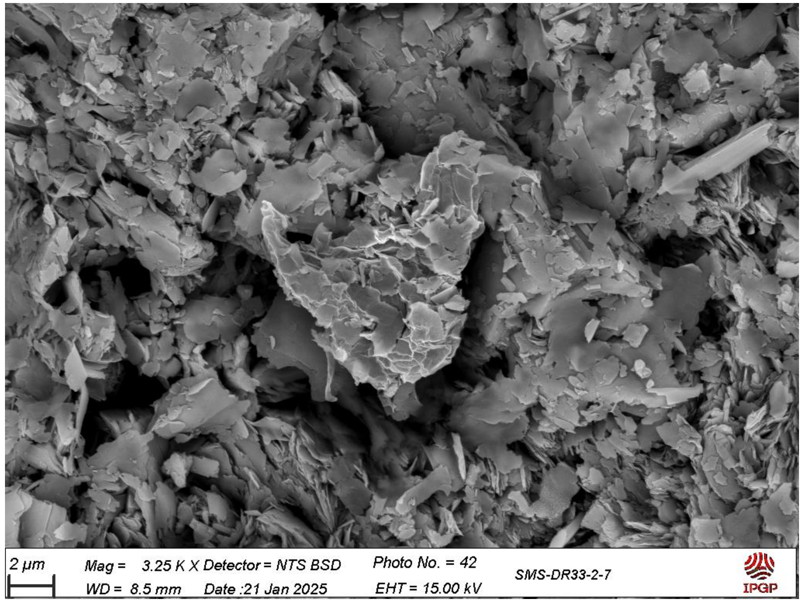

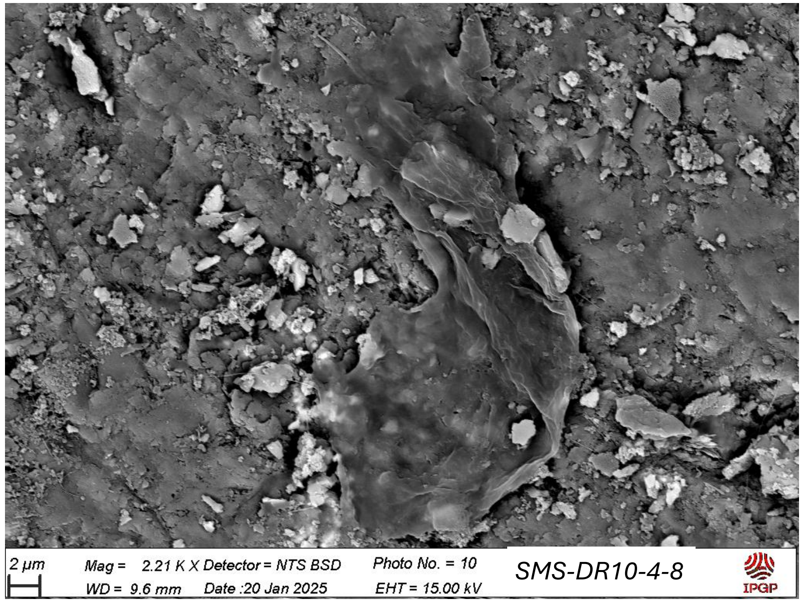

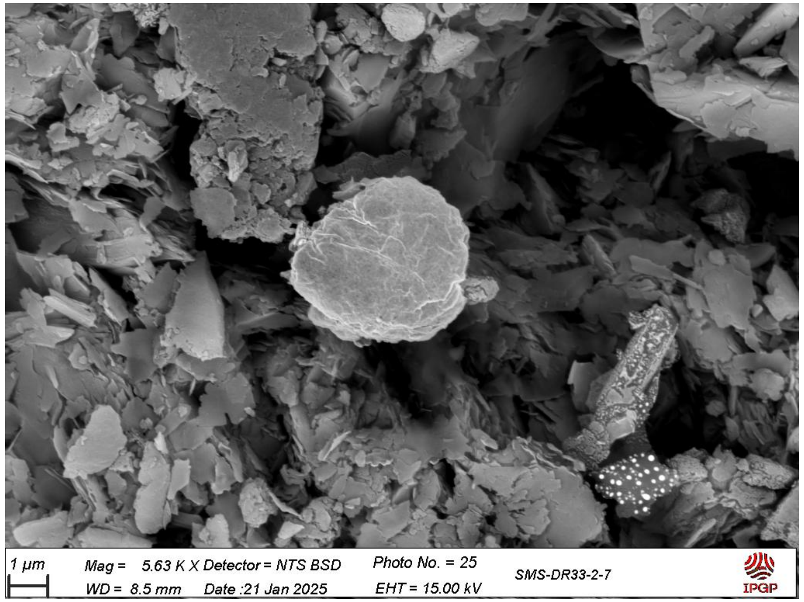

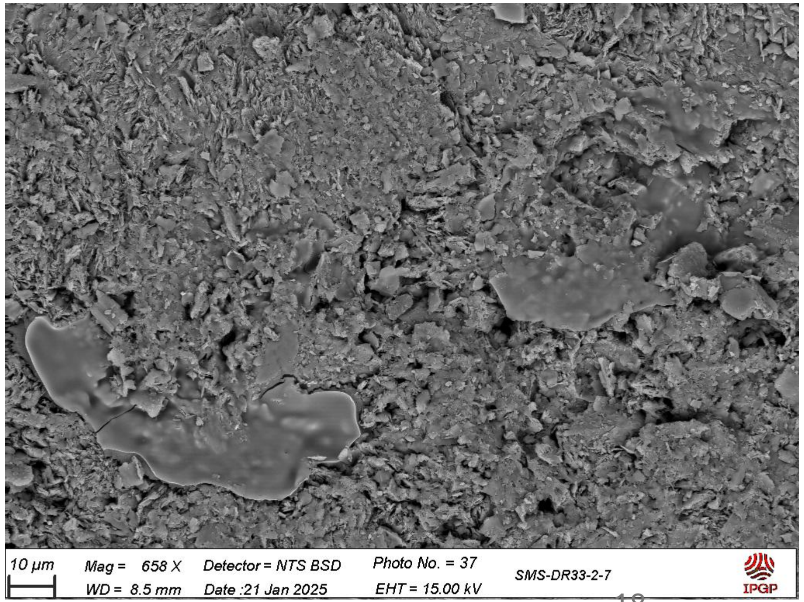

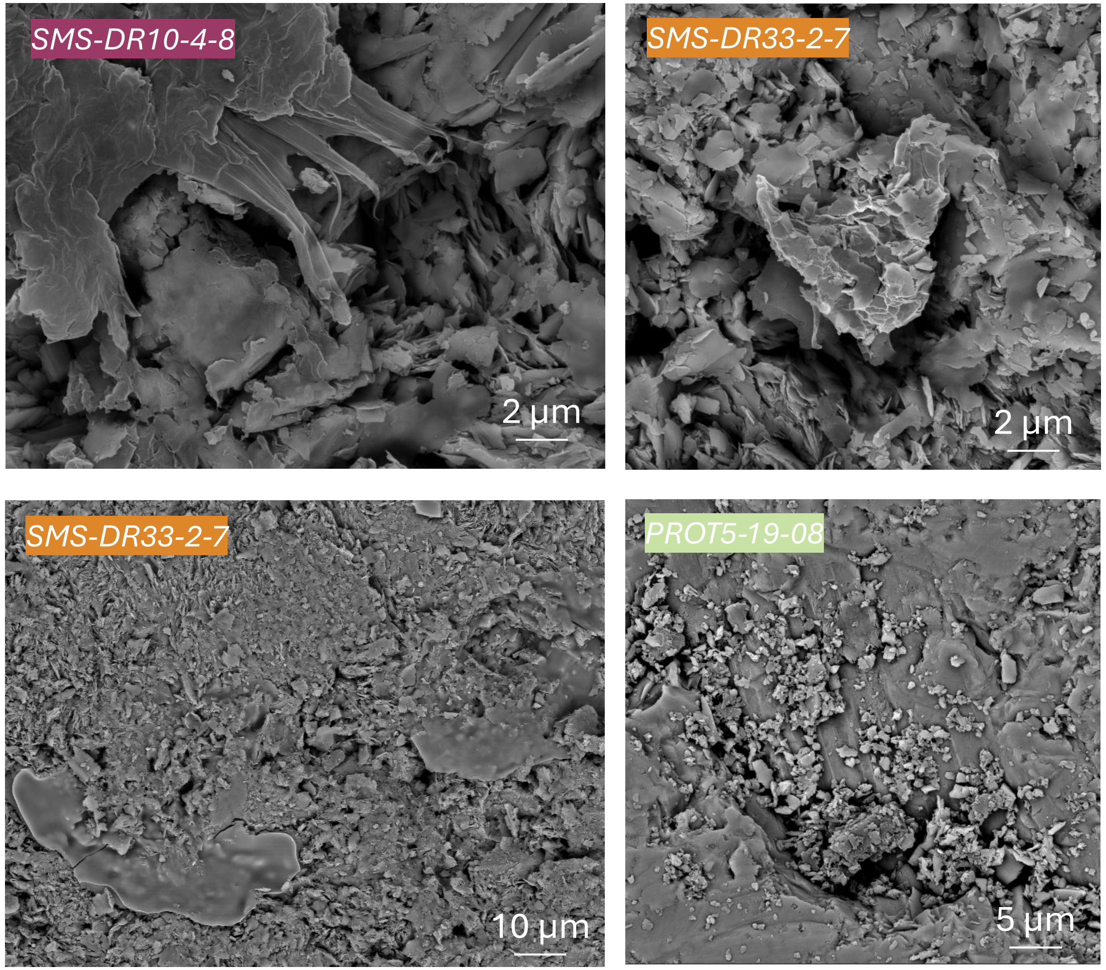
SMS-DR10-4-8
2 µm
SMS-DR33-2-7
2 µm
SMS-DR33-2-7
10 µm
PROT5-19-08
5 µm

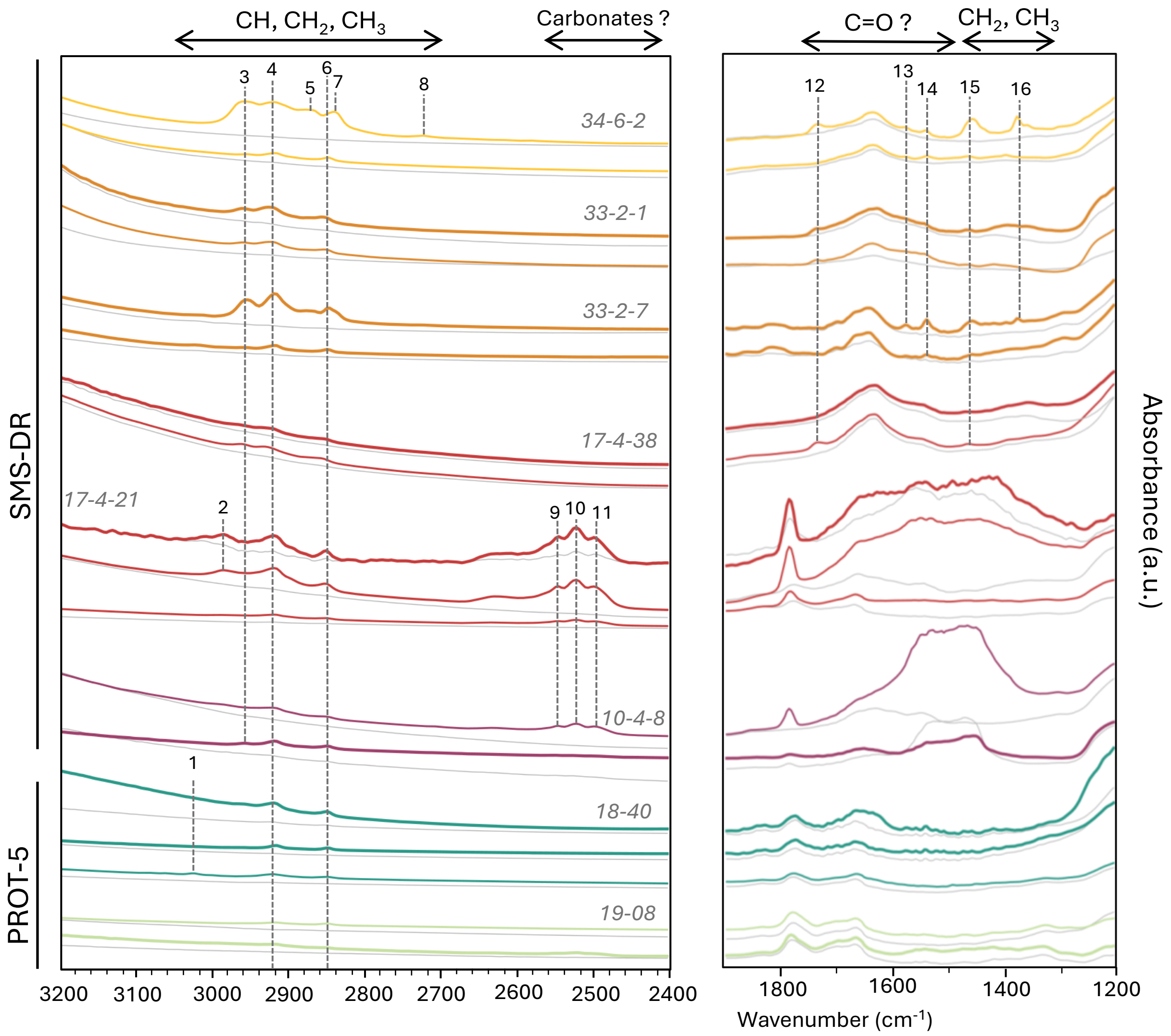
CH, CH2, CH3
Carbonates ?
C=O ?
CH2, CH3
34-6-2
33-2-1
33-2-7
17-4-38
17-4-21
10-4-8
18-40
19-08
SMS-DR
PROT-5
Absorbance (a.u.)
Wavenumber (cm-1)
3200 3100 3000 2900 2800 2700 2600 2500 2400
1800 1600 1400 1200

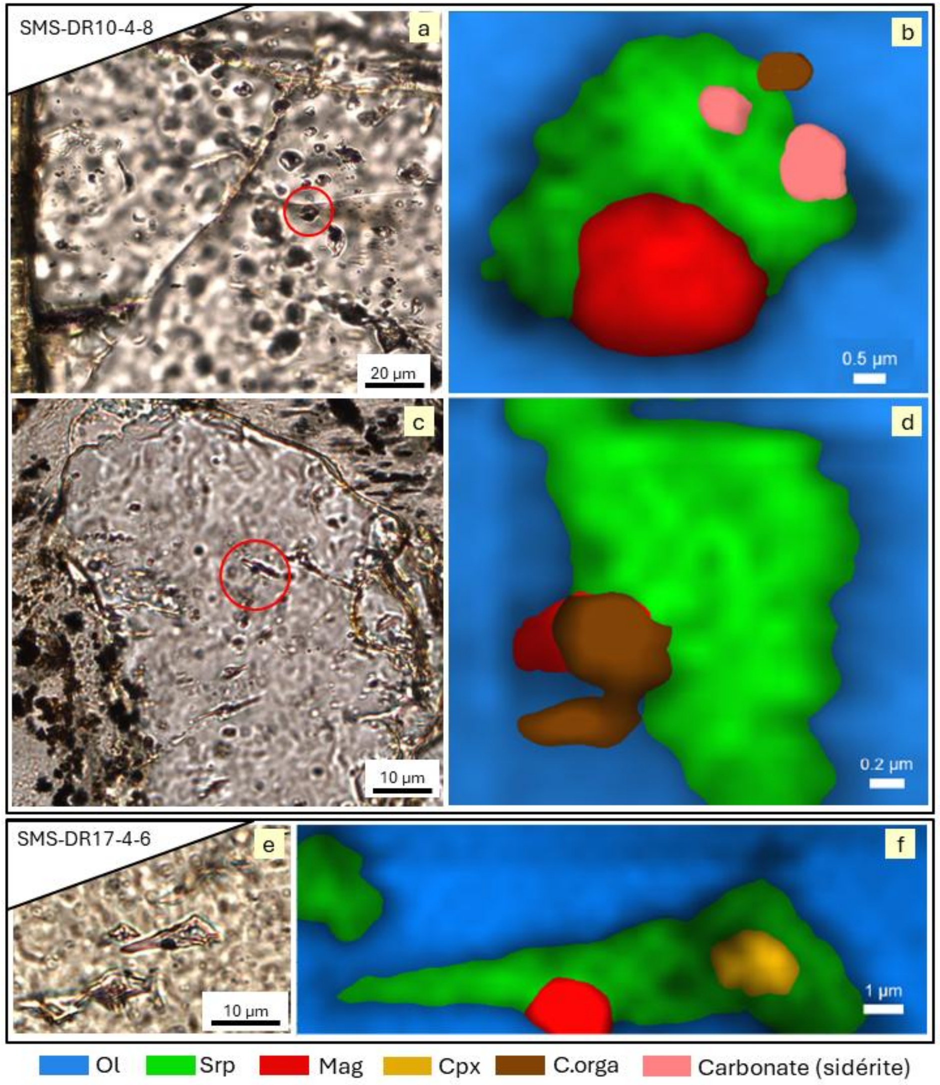
SMS-DR10-4-8
a
20 µm
b
0.5 µm
c
10 µm
d
0.2 µm
SMS-DR17-4-6
e
10 µm
f
1 µm
Ol
Srp
Mag
Cpx
C.orga
Carbonate (sidérite)

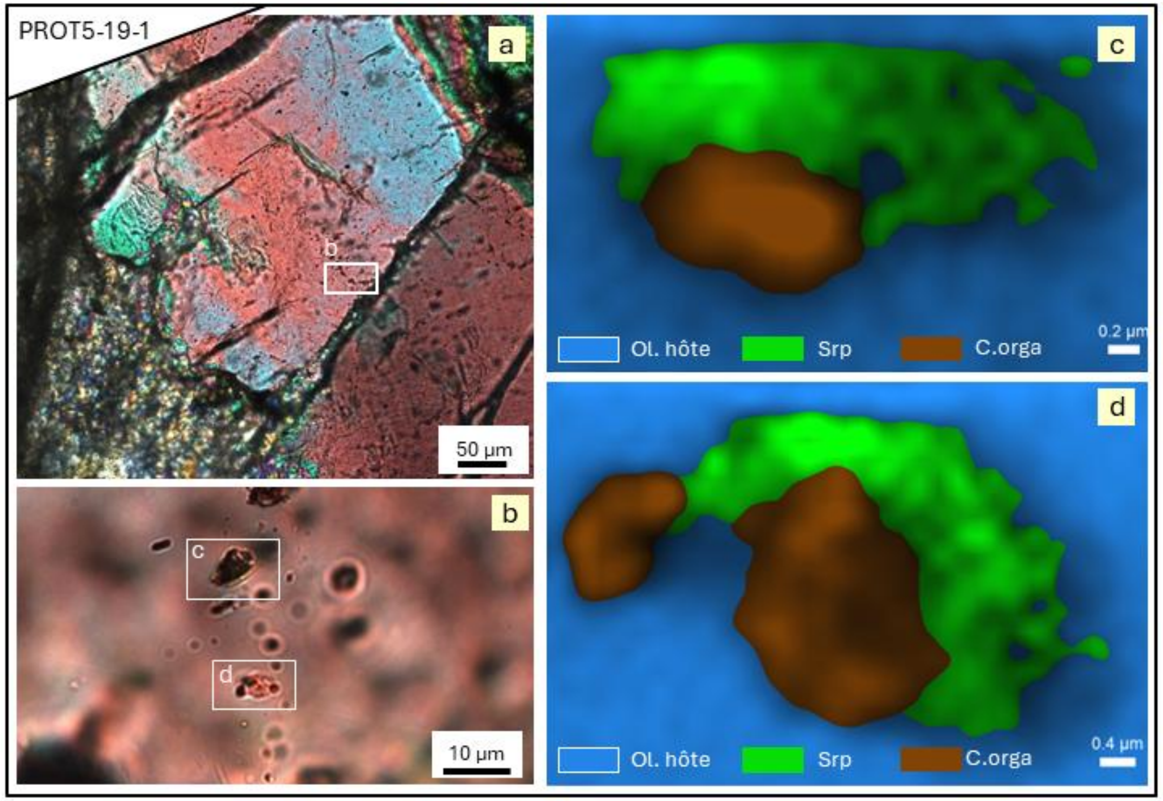
PROT5-19-1
a
50 µm
b
10 µm
c
Ol. hôte
Srp
C.orga
0.2 µm
d
Ol. hôte
Srp
C.orga
0.4 µm